International Journal of Mass Spectrometry 464 (2021) 116574

Contents lists available at ScienceDirect

International Journal of Mass Spectrometry

journal homepage: www.elsevier.com/locate/ijms

Full Length Article

A quantitative light-isotope measurement system for climate and energy applications

Robert P. Thorn Jr. [a,*], Andrew K. Gillespie [a], Cuikun Lin [a], Heather Higgins [a], Shelby Lacouture [a], Robert Baca [a], Baudilio Tejerina [b], Andrew A. Durso [a], Django Ian Jones [a], Ruth Ogu [a], Brett Neurohr [a], Trevor Dardik [a], Robert V. Duncan [a]

[a] Center for Emerging Energy Science, Department of Physics and Astronomy, Texas Tech University, Lubbock, 79409, TX, United States
[b] Geophysical Fluid Dynamics Laboratory, Office of Oceanic and Atmospheric Research, Princeton University, Princeton, 08540, NJ, United States

ARTICLE INFO

Article history:
Received 19 November 2020
Received in revised form
25 February 2021
Accepted 1 March 2021
Available online 13 March 2021

Keywords:
Quantitative helium isotope analysis
High resolution mass analysis
Compact
Sensitive FT-ICR
Atmospheric noble gas determination
Novel sample purification
Hydrogen purification

ABSTRACT

We describe the design, operation, and performance of a new instrumental configuration capable of quantitative determinations with sub-picomole accuracy of dilute concentrations of low mass species, such as ^{4}He, ^{3}He, ^{20}Ne, and ^{40}Ar, in a balance of stable hydrogen (H_2, DH, and D_2) gas. This inexpensive system may realize important applications in fields ranging from climate studies to hydrogen fusion energy research, thereby providing an expanded availability of this diagnostic within emerging energy systems research and development. These spectra, calibration curves, and determinations were obtained by using a novel method for the purification and subsequent removal of the hydrogen matrix gas, and an extensively modified commercial Fourier Transform Ion Cyclotron Resonance (FT-ICR) mass spectrometer with an electron impact (EI) ionizer. These high-resolution FT-ICR mass spectrometers have routinely achieved a resolution, $R = m/\Delta m$ better than 10,000 Da at mass-3, with a mass resolution that scales as 1/m. These devices have easily resolved D_2 from ^{4}He, and DH from ^{3}He. The performance of this upgraded instrument has demonstrated the ability to detect impurities from tiny air leaks, such as ^{40}Ar and ^{20}Ne, in the presence of the hydrogen matrix gas. While no concentration measurements of radioactive species have been attempted to date with this system, it is expected to easily resolve DT from D_2H (a 0.0059 Da mass difference) and HT from all other mass-4 species.

1. Introduction

We report on a new measurement system based upon an inexpensive, custom-modified Ion-Cyclotron Resonance Mass Spectrometer (ICR-MS) that is capable of quantitatively measuring sub-picomole amounts of ^{4}He and ^{3}He in a hydrogen gas background. This measurement system is based upon a highly-modified 'Quantra' ICR-MS that was last sold by Siemens Industry, Inc. (Process Analytics) in 2008, two of which we obtained from used equipment marketers. We describe commercial, off-the-shelf (COTS) modifications to these Quantra units that expand their capabilities into this low-mass range. The resulting system exhibits adequate resolution and quantitative measurement capabilities to contribute significantly as a diagnostic tool within climate and energy research. The linearity and stability of this system is demonstrated through repeated periodic calibrations against a known dilute helium-in-balance-hydrogen external standard. Numerous similarly-designed systems were calibrated and compared to demonstrate unit-to-unit variability. This system has also been used to measure ^{40}Ar and ^{20}Ne quantitatively, and these measurements have provided real-time air invasion detection into the sample and/or measurement system while helium measurements were being made. As discussed in detail below, for accurate quantitative measurements of light ions, such as helium, it is essential that the partial pressures of all other atoms and molecules be reduced to exceptionally low levels, permitting ultra-high vacuum conditions to be maintained in the ICR mass spectrometer. In order to develop an accurate method of measuring sub-picomole levels of helium in a balance of hydrogen gas, it was essential to measure sample volumes and pressures accurately, and then to remove virtually all of the hydrogen matrix gas before the

* Corresponding author.
E-mail address: peyton.thorn@ttu.edu (R.P. Thorn).

https://doi.org/10.1016/j.ijms.2021.116574

quantitative mass spectrometry measurement of the helium was made. The helium impurity levels within the hydrogen matrix gas must be reduced to less than 0.001 ppm to avoid quantitative systematic errors, and this required improvements in hydrogen gas purification technology that are described herein. Applications that require accurate light isotope measurements are discussed first in this introduction. This is followed by an introduction to the quantitative approach to measuring very small levels of helium in balance hydrogen using calibrated external manifolds. Then our modified Ion − Cyclotron Resonance (ICR) method of mass spectrometry measurement is introduced, and measurements and the stability and the unit-to-unit variation are documented in detail.

1.1. Applications of this technique

Accurate determination of the abundance of light-atom concentrations in the Earth's atmosphere is an important application of the technology discussed herein. Such measurements are important to the study of the Earth's dynamics, and potentially to timely planetary concerns, such as the study of climate change. The abundance of two stable noble gases within the Earth's troposphere, helium and neon, was initially measured using quantitative separation by fractional absorption in 1946 [1]. The currently accepted (1976) standard atmospheric composition has a helium concentration of 5.24 ppm by volume [2]. This helium composition is a balance between generation from alpha decay within the Earth's radioactive core, input from the solar wind at the poles, and subsequent degassing and thermal escape from the upper atmosphere [3,4]. Nonthermal escape of helium has also been observed [4,5]. The neon concentration in the atmosphere is 18.18 ppm by volume, of which 90.48% of this neon concentration is the isotope ^{20}Ne, 0.27% is ^{21}Ne, and 9.25% is ^{22}Ne [2].

The accurate determination of the ratio of the stable helium isotopes, ^{3}He/^{4}He, is of current interest in the Earth's troposphere [6–14]. This interest was initiated by a study that showed that there was a possible rate of change in the air ^{3}He/^{4}He ratio due to anthropogenic activity, mainly the release of ^{4}He through the exploitation of fossil fuels [6]. However, these initial reported results have not realized wide-spread acceptance by the scientific community, but they remain a topic for further study. Using a high-resolution magnetic sector mass spectrometer, other researchers concluded that there was no change in the atmospheric helium isotope ratio [15,16].

Another source of ^{3}He within the atmosphere is the beta emitting decay of tritium, ^{3}H, which has various sources on Earth. Anthropogenic tritium sources include nuclear power-plants, and residual levels from earlier nuclear weapons testing. The natural cosmogenic source of tritium originates in the upper troposphere and the lower stratosphere. Another natural ^{3}He source is deep-earth radioactive decay.

Similarly, the accurate determination of the ratio of the neon isotopes, ^{21}Ne/^{20}Ne is of current interest in the Earth's troposphere [17–20], and the techniques discussed herein may be readily expanded to measure and study the ^{21}Ne/^{20}Ne ratio in the atmosphere.

Researchers studying hydrogen fusion have also used mass spectrometry in efforts to detect the two stable helium isotopes as a gaseous product of the nuclear reactions. These experiments required an instrument with very high sensitivity, in addition to a high resolving power. Early attempts to detect and resolve the helium isotopes and other low mass species were based on the use of two-quadrapole mass spectrometers (QMS) [21]. Other helium measurements were performed using a double focusing 90°magnetic sector instrument [22–26]. An omegatron ICR mass spectrometer with a high magnetic field has been in use at the Alcator C-Mod tokamak magnetic fusion device for sampling the plasma [27,28]. An ultra-high resolution quadrapole mass spectrometer, the Hiden DLS-20 (Hiden Analytical Ltd., Warrington, Cheshire, UK) has been specifically designed for the analysis of hydrogen and helium isotopes and applied toward fusion research at the Joint European Torus (JET) tokamak [29]. It used a threshold ionization mass spectrometry mode [30], in which the accurate emission control of the ion source electrons was performed, so that the DLS-20 discriminated between D_2 and ^{4}He. A similar quadrapole mass spectrometry method has been used at the DIII-D26, EAST and the HT-7 tokamaks [31,32].

Other users for high resolution, low mass spectrometry include national nuclear weapons laboratories within the U.S. Department of Energy [33]. In this case, a Fourier Transform, Ion Cyclotron Resonance (FT-ICR) mass spectrometer instrument, very similar to the one described here, performed measurements for monitoring the separation of hydrogen, deuterium, tritium, and helium. Prior to the use of the FT-ICR instrument within national laboratories, magnetic sector mass spectrometers, such as a Thermo Finnigan MAT series mass spectrometer was used for hydrogen isotope ratio monitoring [33–35].

The identification and quantification of an analyte, especially in the presence of other analytes, is a primary goal of mass spectrometry. We focus on the primary benefits of this ICR mass spectrometer when coupled to a manifold designed for removal of interfering species. They are: 1) the ultrahigh mass resolving power at low masses, 2) the mass accuracy that is obtainable at low masses, and 3) the very low analytically determined detection thresholds and subsequent improved measurement concentration levels that are obtainable.

1.2. Description of the modified Quantra FT-ICR mass spectrometer

We have substantially upgraded a commercial, compact, and high-resolution FT-ICR mass spectrometer, named the Quantra, that was manufactured by Siemens Analytical Products and Solutions [36]. Although the manufacture of this instrument has been discontinued, it remains available today on the used equipment market. It provided the user with a very high-resolution mass spectrum from which the identification and quantification of the sample components were obtained. Unlike most FT-ICR instruments that use strong, massive magnets for large molecule analysis, the Quantra uses a smaller 0.9 T field strength permanent magnet. This was better suited for confining the volatile, lower mass ions, and it utilized modest voltages for low mass ion control. It was originally designed for measuring the mass range of 12–1000 Da, but we modified it to extend its measurements into the mass range of m/z = 1 to 12. We are currently replacing the remaining legacy technology of the Quantra design with updated, state-of-the-art measurement technology that may be readily digitally reconfigured to optimize custom measurements. Another compact FT-ICR mass spectrometer is manufactured by AlyXan (Centre Hoche, 3 rue Condorcet, 91260 Juvisy sur Orge, France) and is now commercially available. It uses a Halbach array 1.5 T permanent magnet [37,38]. It is based upon an earlier design that used a 1.24 T field strength permanent magnet [39].

The original maximum 5 MHz data collection and pulse frequency limited the measurement to masses above 12 Da. The instrument mass resolution was $m/\Delta m$ = 20000 at m/z = 131. The specified mass accuracy was 100 ppm or 0.004 Da at m/z = 28. We have modified it to extend its measurements into the lower mass range of m/z = 1 to 12. There were two major challenges with using

the unmodified Quantra for detection of low m/z species: First, the 5 MHz A/D converter sampling rate limited direct-mode detection to species with cyclotron frequencies less than the corresponding Nyquist limit of 2.5 MHz which corresponds to about m/z = 5.6, so much higher excitation frequencies were required to extend this detection range to lower values of m/z. This higher excitation frequency was provided by using a replacement arbitrary waveform generator (AWG), Model DG1062Z from Rigol Instruments, as described in the supporting information. Secondly, the original data acquisition and control hardware and software that was provided with the original Quantra performed well at this extended frequency range, which was above its original designed range. Hence, we have continued to use the original Quantra software, which was written in a proprietary scripting language, to control most of the instrument operating parameters over this extended frequency range. However, the access to the critically timed events, such as in triggering data acquisition, was needed. These modifications to the timed events are also described in the supporting information.

2. Experimental

2.1. Overview of the vacuum system, sample purification, and manifold operation

An internal diode element sputter-ion pump established the ultra-high vacuum conditions in the ICR cell. Ultra-high vacuum was a key required parameter so any ion-molecule reactions and ion-neutral collisions that dampened the coherent ion motion were minimized. This was especially crucial for helium ions because their ionization potential of 24.59 eV, which is the highest of any element [40], enabled rapid charge exchange reactions with any residual atoms or other gases present in the FT-ICR cell.

Limiting the concentration of molecular nitrogen and other gaseous species in the ICR cell results in a higher and more stable helium cation population, resulting in a larger, more repeatable signal. A sample preparation technique that removes the lower molecular weight gaseous species was the key to obtaining an accurate helium determination without systematic errors.

2.2. Description and operation of the manifold system

The Quantra sample inlet system as shown in Fig. 1 included a front end manifold with multiple inlet ports, a sample loop of fixed volume, and a manifold chamber containing the non-evaporable getter (NEG) pump (CF16-MK2-172, SAES Group S.p.A., Milano, Italy), for use before sample injection into the Quantra resonance chamber It also included several pressure transducers, pneumatically operated bellows valves, an activated charcoal cold trap, and a calibrated leak valve.

The NEG pump was used to remove the deuterium 'matrix' gas from the calibration and the sampled gases. This NEG pump utilized a sintered porous getter based on a Zr−V−Fe alloy and had a high pumping speed for H_2 and D_2 [41]. The NEG pump was regenerated under heat and vacuum to restore its ability to absorb hydrogen (protium and deuterium). Other diatomic and triatomic species, such as nitrogen, oxygen, water, and carbon dioxide, were irreversibly absorbed into the alloy, vastly limiting the lifetime of this pump. Hence, if these molecules were present in the sample, a cryopumping procedure using the charcoal cold trap was used to remove these species, thus preserving the activity of the NEG pump.

The LabVIEW program controls the sequence of all pneumatic valve opening and closing, other than valves 8, A, and B and the calibrated leak valve. The procedure used to measure an aliquot of gas follows. Gas was allowed into the front end volume where the pressure was monitored by P1, a MKS 910 dual-sensor transducer. The gas may either be condensed in the cold trap or an aliquot of gas may be allowed into the sample injection volume. The charcoal filled cold trap and cryopumping were used when measuring an unknown gas that might contain high concentrations of Ar, Ne, N_2, O_2, H_2O or other contaminants. The getter manifold was also attached to the turbomolecular pumping station so that the getter material may be baked out and evacuated whenever the hydrogen absorption rate was slow. The FT-ICR instrument was connected to an external ion pump through valve 8 in case maintenance of the ICR cell was required. The manifold operation began when an aliquot of gas was isolated in the front end volume. The aliquot of gas entered the getter manifold where the hydrogen matrix was absorbed by the SAES CapaciTorr getter and helium was left in the headspace gas. After 60 s of dwell time, the pressure reading of P2 was below 1×10^{-5} Torr. Then the remaining headspace gas passes through the calibrated leak valve and enters the FT-ICR. The leak valve knob was set to dispense the headspace gas over a period of 30 s. Table 4 in the supporting information shows the manifold valve timing sequence.

If an initial wide mass spectral scan showed air intrusion into the gas sample bottle, as evidenced by an ^{40}Ar or ^{20}Ne peak, an additional sample purification step was required. This step was also required if the sample matrix was not hydrogen or deuterium, or if the sample was drawn from a moist environment. Although the NEG pump can remove the nitrogen and the oxygen present in air, these species should be removed from the gas sample before being irreversibly absorbed by the NEG pump, which limited its lifetime. This additional purification step was accomplished using a U-tube cold trap that had been added to the sample inlet valve, typically valve 5. Alternatively, it can be inserted between valves 1 and 2 in a bypass configuration. It was filled with activated charcoal and a getter (SAES Group getter type ST707). Once the sample was admitted to this trap, the temperature was reduced to T = 77 K with liquid N_2 and it condensed and absorbed the species with higher boiling points, such as Ar, CO_2, H_2O, N_2, and O_2. H_2 and its isotopes were absorbed primarily by the NEG pump. Ne, He, and their isotopes which have boiling points lower than liquid N_2 were not condensed or absorbed on the charcoal to any appreciable extent [42]. Besides enabling the use of a higher sampling pressure, this additional impurity removal trap also allowed the analysis of the helium concentration within air samples, which served as a calibration fixed-point reference at 5.24 ppm within this work [2].

3. Results and discussion

3.1. Calibration

After a determination of the background levels, the response of the Quantra was calibrated using an external standard of known ^4He or ^3He composition. Either a 30-point, 20-point, or a 15-point calibration for He was performed daily to ensure that there was not a significant drift in the sensitivity. An automated sequence operated the manifold pneumatic valves to load the calibration gas into the injection volume, then into the NEG manifold, and finally into the Quantra inlet port (see Supporting Information). The same calibration procedure described below has been used for the noble gas species that have been analyzed (^4He, ^3He, ^{20}Ne, and ^{40}Ar). The first acquired signal begins with a higher pressure in the front end, typically P = 8−15 Torr when using a nominal 5 ppm He calibration gas. The subsequent data points were obtained as the pressure was reduced through the automated filling of the injection volume.

To ensure that there were not any hysteresis effects, a calibration experiment was performed where the injection volume pressure

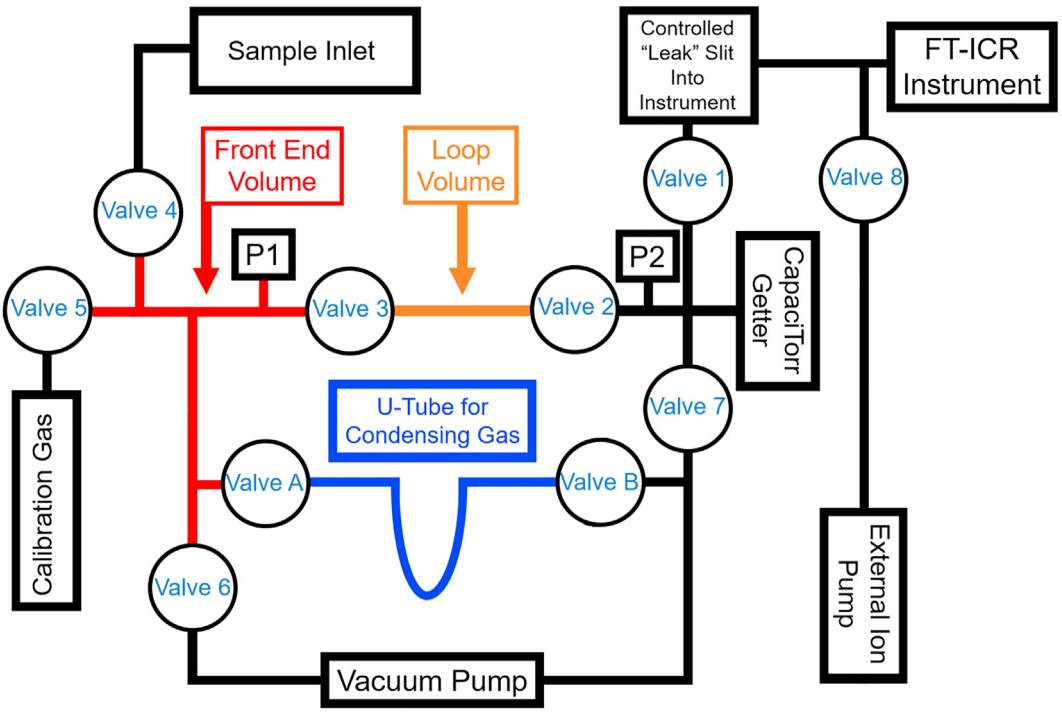

Fig. 1. The Quantra sample inlet system and the pretreatment U-tube cold trap for removal of argon and other species.

was first sequentially decreased, and then sequentially increased. No hysteresis effect was observed. Furthermore, the instrument has been exposed only to noble, monoatomic gases either of atmospheric composition or of commercial calibration gases with concentrations of 10 ppm or less. When the measurements described here were finished, noble gas exposure had occurred for less than 15 months. Because the daily measurements of the background noble gas levels were constant (see Supporting Information), and the instrument was routinely baked at T = 180 °C and evacuated with an appendage turbomolecular pump, instrument 'memory' (i.e. residual helium gas effects) was not observed. Residual hydrogen gas effects were only observed when the CapaciTorr NEG pump was not adequately thermally recycled between runs. Routine bakeouts and the use of the CapaciTorr getter removed any interfering hydrogen species including the potential spectral interferences of $^{1}HD^{+}$ and $^{1}H_{3}^{+}$ which interfered with the $^{3}He^{+}$ signal [43].

To calibrate the instrument, measurements of net signal and loading pressure were gathered for a calibrant gas. For one such instrument, the calibrant gas contained 6.52 ppm ^{4}He in a deuterium balance, as confirmed against the 5.24 ppm of ^{4}He observed in an air sample measurement. The ideal gas law was used along with the known He concentration to calculate the total number of picomoles of He present in the sample loop, V_{SL}. At a given pressure, the total amount of picomoles of gas, $n_{Total(i)}$, in V_{SL} was calculated,

$$N_{total(i)} = \frac{P_i V_{SL}}{RT} \tag{1}$$

and the total number of picomoles of ^{4}He, n_{He}, present was calculated:

$$N_{[He](i)} = \frac{6.52}{10^{6}} n_{total(i)} \tag{2}$$

At a given pressure, a known amount of ^{4}He was allowed into the instrument and the net signal, NS_i, was measured. This process was repeated several times to obtain a linear trend in the net signal as a function of $n_{He(i)}$. This trend was inverted so that the slope and intercept may be used to determine [^{4}He] for an unknown gas sample. Let the calibration slope be denoted m, the calibration intercept be denoted b, and an individual measurement for net signal be denoted NSi. The standard error of the slope is s_m, and of the intercept, s_b. The calibration equation is:

$$n_{He(i)} = (m \pm s_m) \times (NS_i) + (b \pm s_b) \tag{3}$$

Fig. 2 shows the calibration curves for the helium species before the trend was inverted. After inverting the calibration equation, based on linear regression of the ^{4}He data, would be

$$n_{He(i)} = (5.763 \pm 0.045) \times (NS_i) - (0.189 \pm 0.054) \tag{4}$$

Assuming this equation will hold true for any unknown gas sample, one may measure the net signal from the unknown gas sample and calculate $n_{He(i)}$ present in an aliquot of that sample.

3.2. Linear dynamic range, and limit of detection for ^{4}He and ^{3}He

As shown below for the ^{4}He and the ^{3}He calibration gases, the Quantra responds linearly from 0.24 to 19.0 pmol (Fig. 2). From a linear regression analysis of the data points, the calibration curve statistics were determined including the standard error of the slope, s_m, and of the intercept, s_b. The standard error of the intercept gave the error structure used to determine the limit of detection, LOD [44]. Using a 95% confidence limit and the number of data points (degrees of freedom), the two-tail critical t-value, t_{crit}, was first determined. From this value, the LOD[He] was determined:

$$LOD[He] = (t_{crit} \times s_b)/b \tag{5}$$

For the data in Fig. 2, the limits of detection, LOD, were 0.12 pmol

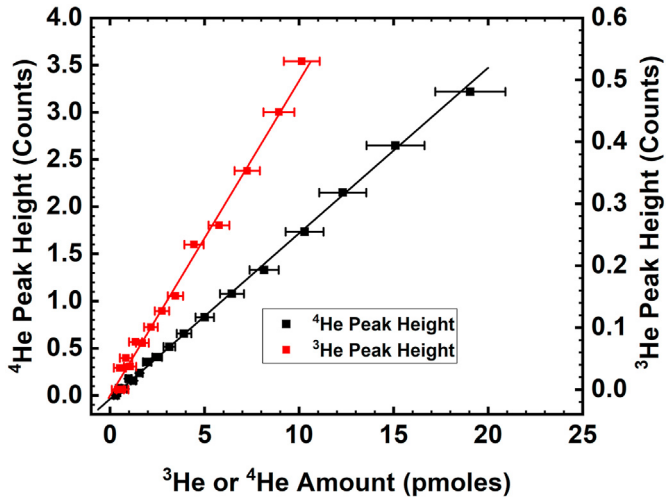

Fig. 2. Typical calibration measurements showing the net signal versus the sample amount of ^{4}He and ^{3}He. The ^{4}He and ^{3}He calibration gases had concentrations of 6.52 and 5.76 ppm respectively.

^{4}He and 0.25 pmol ^{3}He. Next, the Lowest Level of Quantification, LLOQ, values were determined using the International Conference on Harmonisation (ICH) factor of 10:

$$LLOQ[He] = (10 \times s_m)/m \quad (6)$$

For the data in Fig. 2, the lower limit of quantification was 0.555 pmol ^{4}He, which was typical of measurements taken at various times on different machines. The LOD and the LLOQ varied between the different Quantras and they were also dependent upon the species measured. Table 1 below shows the values obtained for four of the instruments when a ^{4}He calibration gas was used. Once a calibration trend has been obtained, the unknown gas sample was allowed into the front end volume, V_{FE}. The pressure was recorded and used with the ideal gas law to calculate the total amount of the unknown gas, $n_{(total(j))}$. The gas was purified by exposing the gas to a cold trap filled with charcoal and ST707 getter material. Gas species with low boiling points remain in the headspace gas. Any remaining headspace gas was allowed into the instrument for measurement.

This measurement was repeated for the aliquot of gas until the amount of ^{4}He in the headspace gas falls below the lower limit of quantification. The amount of ^{4}He present in the gas aliquot admitted to the instrument for each jth measurement was calculated using the net signal with the calibration equation (Eq. (7)). Summing the amount of ^{4}He from these measurements, the $n_{[He](j)}$ values, yielded the total amount of ^{4}He inside the unknown gas sample. The loading pressure was used with the ideal gas law to determine the total moles in the gas aliquot prior to condensing.

Table 1
^{4}He Calibration results for four FT-ICR mass spectrometers.

Parameter	Quantra 1	Quantra 3	Quantra 4	Quantra 6
No. of Calibrations for ^{4}He	474	254	76	35
Average Slope, Counts/pmole	0.286	0.165	0.333	0.142
Average Intercept, Counts	0.0087	-0.022	0.053	0.079
Average LOD, pmole	0.162	0.184	0.141	0.185
Average LLOQ, pmole	0.715	0.818	0.659	0.891

This amount of gas includes all gas species in V_{FE} whether it be ^{4}He, D_2, H_2, or any impurities. Let this amount of gas be denoted $n_{total(j)}$. The ratio of the total amount of ^{4}He to n_{total} yields the concentration of ^{4}He in the unknown gas sample, denoted as [He]:

$$[He] = \frac{\sum n_{[He](j)}}{n_{(total)(j)}} \times 10^6 \quad (7)$$

To test the lower limits of the instrument's capabilities, this experiment was repeated on an ultra-purified deuterium gas sample. A description of the purification system and method is given in the Supporting Information. This system resulted in an extremely pure hydrogen gas with literally no moisture or oxygen carry over. A purity more than 99.9999995% (eight 9s) was routinely obtained. The research grade supply gas was tested before and after this purification process.

The set of ^{4}He measurements presented in Fig. 3 were made on three separate aliquots of research grade deuterium gas after purification. The measurements were conducted using between 622 and 947 μmol of total gas resulting in an average concentration of 4.0 ± 1.3 ppb ^{4}He in the ultra-purified deuterium gas. The concentration of ^{4}He in the research-grade deuterium gas was 44 ± 5 ppb before the absorption-based purification procedure. The purification process was successful in removing over 90% of the residual ^{4}He present in the original research-grade supply gas.

3.3. Detection and resolution for ^{3}He

Experiments were performed using a 5.76 ppm ^{3}He calibration gas in a DH matrix to illustrate the excellent resolution obtained using the upgraded Quantra. As shown below in Fig. 4, the ^{3}He, DH, and H_3 signals are well resolved as are the ^{4}He and D_2 signals. Notice also that the H_3 peak, which is only 0.00155 Da above the DH peak, is clearly resolved. The resolution of the ICR mass spectrometer is about 0.0003 Da in Fig. 4, resulting in a resolving power in excess of 10,000 in this mass range.

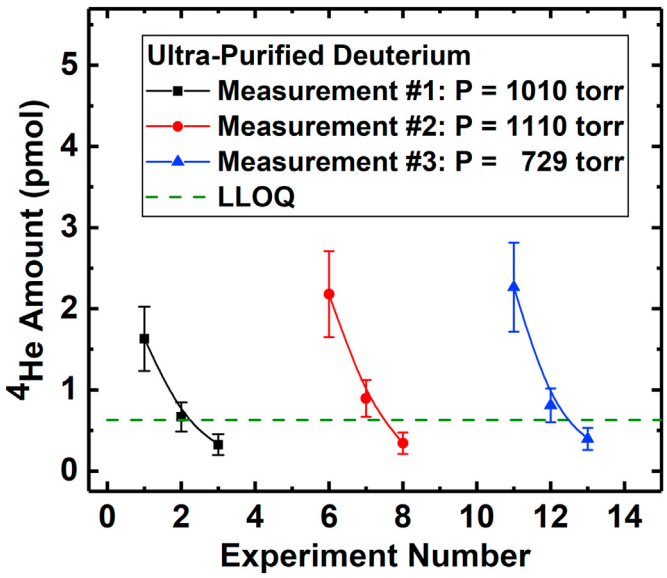

Fig. 3. Calculated ^{4}He amount versus measurement iteration number for three aliquots of the ultra-purified deuterium gas.

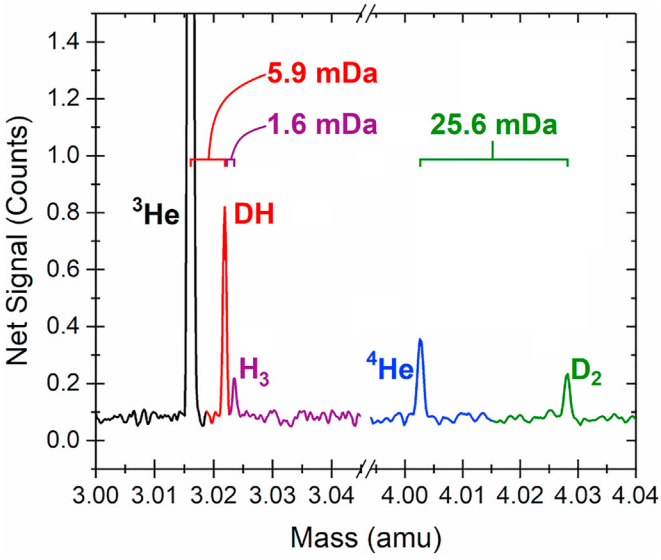

Fig. 4. Illustration of Quantra's resolution at low mass. The excitation frequencies were 4.828 MHz and 4.8235 MHz for ^{3}He and DH, respectively. The frequencies were 3.487 and 3.508 MHz for ^{4}He and D_2, respectively. Notice that the H_3 peak at 0.0015 Da above the DH peak is clearly resolved, demonstrating the instrument's mass resolution.

3.4. Calibration, linear dynamic range, and limit of detection for Ar and Ne

Similar calibration curves, shown in Fig. 5, have also been obtained for ^{40}Ar and ^{20}Ne. For the same EI source settings, the sensitivity increased with the mass of the analyte gas. This was primarily due to the effective ionization cross section [45]. However, for the Quantra the sensitivities for these two species were similar to that for ^{4}He. It should be noted that the internal ion pump had a significantly slower pumping speed for Ar and Ne, and thus a waiting period of greater than 5 min was required between the acquisition of the data points. This was expected as helium has a different pumping mechanism than the heavier noble gases [46]. As

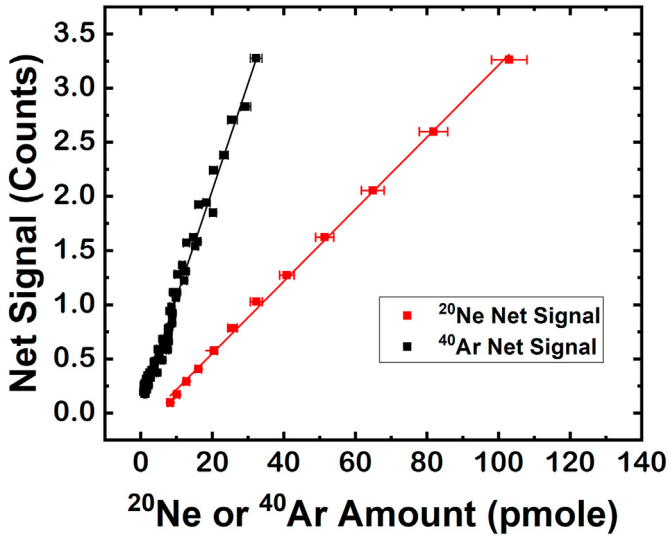

Fig. 5. Measured net signal versus the amount of argon or neon. The black data points and regression line were obtained using the 5.02 ppm Ar gas in balance H_2. The red data points and regression line were obtained using the 5.06 ppm Ne gas in balance H_2 and the cold trap.

with ^{4}He, the calibration curves were obtained using an external calibration gas and an electron beam energy of 70 eV. With ^{4}He cations generated by a Nier-type ion source, the ionization efficiency peaks at 70 eV [47]. A typical LLOQ for ^{40}Ar was 1.14 pmol and for ^{20}Ne was 1.48 pmol.

For quantitative analysis of ^{20}Ne at m/z = 19.9924, it was critically important to avoid potential isobaric interferences [17–20], i.e., isotopes that share a common mass. For ^{20}Ne, a significant interference was the detection of $^{40}Ar^{+2}$ at m/z = 19.9812, which was only 0.0112 Da lower. Peak separation required a resolution of 1777 [17,18] which was not attainable at this mass range by the modified Quantra. This interfering $^{40}Ar^{+2}$ signal was measured with the same frequency ($f = 7.0 \times 10^{5} Hz$) as the ^{20}Ne signal and with a 70 eV electron beam used to ionize the gases. Residual argon background signal has been detected in many mass spectrometers after it has desorbed from flight tubes and ion sources [48]. If both gases are routinely analyzed by the same mass spectrometer, ^{40}Ar will interfere with the ^{20}Ne measurement, especially if the amount of ^{20}Ne is small and the mass spectrometer is operated in static mode. Typically, argon can be separated from neon by a cryogenic trap [49]. Thus, with the EI energy setting at 70 eV, the cold trap was required to remove any ^{40}Ar present in the sample and to obtain an accurate determination of ^{20}Ne. A single stage cold trap was used, rather than a two stage charcoal trap system [49]. It was held at liquid nitrogen temperatures. Another option to prevent interference from $^{40}Ar^{+2}$ was to reduce the energy of ionizing electrons in the ionization source. However, the instrument sensitivity suffers, and the instrument must be recalibrated for all species at the new ionization beam energy. Four other isobaric interferences for ^{20}Ne are possible, $H^{19}F$, $C_3H_4^{+2}$, $D_2^{16}O^{+}$, and $H_2^{18}O^{+}$, which can be removed only with the use of a cold trap.

Although ^{21}Ne measurements have not been performed, one expected isobaric interference was due to $^{20}Ne\text{-}H^{+}$ [17–20]. Quantitative ^{20}Ar determinations were made in the presence of ^{20}Ne without interference. Isobaric interferences for ^{40}Ar, such as $^{200}Hg^{+5}$ and $C_3H_4^{+}$ were absent. It was also determined that the signal from $^{+5}Ne^{+5}$, does not appear at the ^{4}He resonance frequency.

As previously mentioned, this instrument has excellent resolution at lower mass ranges. Experiments have shown that for ^{20}Ne at m/z = 19.9924 the FWHM resolution was 0.031 Da. It increases to 0.122 Da for ^{20}Ar, which agrees with theory.

Linearity and dynamic range were determined for all 3 noble gas species. Linearity for ^{4}He was determined up to 28 pmole. This calibration linearity was observed in the 3 other similar instruments. Linearity for ^{20}Ne was determined from 6 up to 114 pmole and for ^{40}Ar from 0.7 up to 32 pmole.

3.5. Atmospheric air analysis of ^{4}He

Ambient atmospheric air was used to verify the composition of the ^{4}He calibration gases. The residence time of ^{4}He in the Earth's troposphere is approximately 106 years [50], which is significantly longer than the mixing time [51]. Thus, on this basis of a very stable, well mixed composition, most laboratories which are engaged in ^{4}He isotope measurements use atmospheric ^{4}He as an isotopic standard [52]. The set of ^{4}He measurements presented in Fig. 6 were made on 36.3 μmol of air resulting in 182 pmole of ^{4}He and

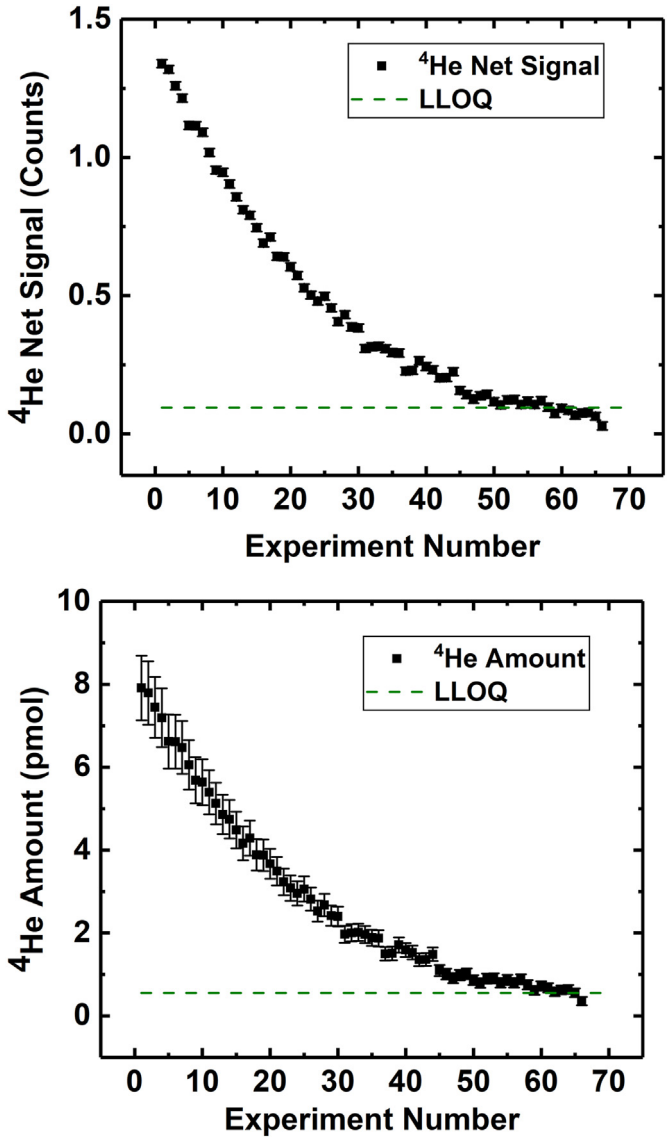

Fig. 6. (Top) Measured net signal versus measurement iteration number. (Bottom) Calculated ^{4}He amount versus measurement iteration number for an aliquot of air.

a concentration of 5.0 ± 0.5 ppm ^{4}He in air [2]. This result was commensurate with the known concentration of 5.2 ppm ^{4}He in air. This measurement method slightly underestimated the ^{4}He concentration of an unknown gas sample because measurements were only iterated until the ^{4}He amount decreased below LLOQ. Any residual ^{4}He gas below LLOQ was left unmeasured inside the front end and U-tube volumes. This demonstrates that the instrument was capable of quantifying ^{4}He concentrations ranging from the 5.24 ppm found in air down to extremely low concentrations on the order of parts per billion.

3.6. Air invasion analysis and efficacy of a layered cryotrap

Numerous additional experiments were performed to characterize the efficacy of the layered U-tube cryotrap as a sample pretreatment method. As discussed in detail above, this additional pretreatment step was necessary when unintentional air invasion into a gas aliquot occurred, or when samples were taken from a wet aqueous sample environment.

These linearity and dynamic range experiments used four different Air/He/H_2 mixtures that contained 0.00, 0.50%, 1.00%, and 1.50% air. All four samples were prepared from as-delivered hydrogen gas that contained 0.479 ppm ^{4}He. After their make-up manometrically, they were allowed more than 24 h of additional mixing time before use to ensure homogeneity.

For this series of experiments, the mass spectrometer operating parameters were optimized for highest sensitivity and then not changed. Additional high mass scan background measurements insured that no air was present in the regulators, in the transfer lines, or in the manifolds. Daily calibration with a 5.2 ppm ^{4}He calibration gas in deuterium matrix showed no significant time dependent change in sensitivity. The first set of experiments consisted of injecting aliquots of these four different gas mixtures into the modified Quantra ICR mass spectrometer and not using the layered cryotrap.

The net ^{4}He signal was determined as a function of sample pressure. Initially, the net signal increased linearly until non-linearity was observed. At this point, an oscillatory magnetron waveform was observed in the time-domain signal. Allowing additional time for reaction equilibrium with the CapaciTorr getter did not significantly increase the upper pressure limit of the linear regime. The results showed that the onset of non-linearity occurred in direct relationship to the concentration of air introduced within the mixtures. This relationship provides a very useful, independent indication at the time of measurement of air invasion into samples, providing a run-time diagnostic to detect tiny leaks in samples that were initially thought to have been hermetic. Such a real-time indication of tiny leaks into samples at the time of test may be a very useful quality control feature of this method.

The second set of experiments included both the CapaciTorr getter and the layered cryotrap, cooled with liquid nitrogen, for the pretreatment of these gas mixtures before injection. The signal linearity (dynamic range) increased substantially when the layered cold trap was used as the results in Table 2 show. By using the calibration curve, along with the volume and temperature of the sample aliquot, the [^{4}He] can be determined using the ideal gas law. There was very good agreement between the actual [^{4}He] and the measured [^{4}He] values when the layered cryotrap was used. As a self-consistency check, Fig. 7 shows an extrapolation of the linear curve fit of the measured [^{4}He] as a function of the air content of the gas mixture. The intercept value of 0.482 ppm shows excellent agreement with the actual value of 0.479 ppm ^{4}He.

3.7. Comparison with commercial instruments

High sensitivity and high precision mass spectrometers that are applicable for noble gas analysis typically are magnetic sector instruments operated in a static mode, i.e., with the vacuum pump turned off, which improves the sensitivity [53]. Numerous noble gas mass spectrometers are commercially available: the NGX600 (Isotopx Inc., Chapel Hill, NC), the Noblesse HR (Nu Instruments, Wrexham, UK), and the three different purpose built instruments from ThermoFisher: Helix SFT Plus, Argus, and the Helix MC (ThermoFisher Scientific, Waltham, MA) [45]. These all utilize a low volume design and a variety of detector modules including Faraday cups and secondary electron multipliers. All 3 instruments have a mass range from 1 to over 140 Da. The Helix SFT Plus has a 120°magnetic sector with a dedicated 90°energy filter for the $^3He^+$ channel. The NGX600 uses a 90°magnetic sector, while the Noblesse uses a 75°magnetic sector. These high-resolution mass spectrometers can now resolve the $^{20}NeH^+$ isobaric interference to

Table 2
Comparison of dynamic ranges for ^{4}He measurements with and without the layered cold trap.

Air Content, %	Maximum Pressure (CapaciTorr only), Torr	Measured [^{4}He], ppm (with Cryotrap), ppm	Measured [^{4}He] (CapaciTorr only), ppm	Actual [^{4}He] (with Cryotrap), ppm	Actual [^{4}He] ppm
0.000	>80	>80	0.453	0.479	0.479
0.500	18	>55	0.529	0.509	0.505
1.000	12	>42	0.925	0.550	0.527
1.500	6	>65	1.685	0.571	0.550

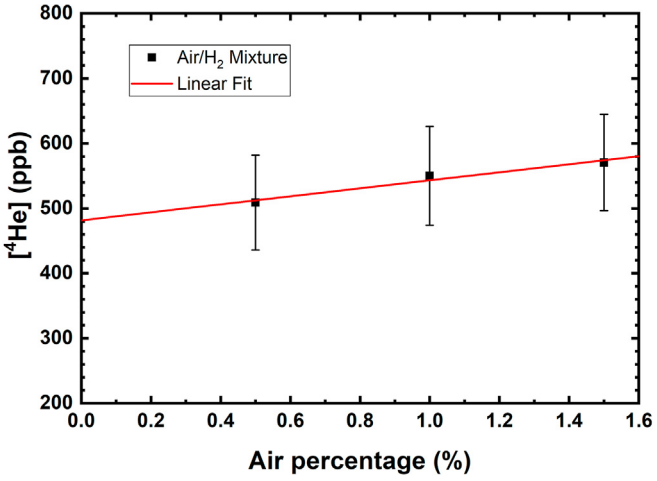

Fig. 7. Extrapolation of the measured [^{4}He] as a function of the air content of the gas mixture. The intercept value was 0.482 ppm.

$^{21}Ne^+$ as well as the ^{20}Ne isobaric interferences [18]. Older magnetic sector instruments, such as the VG 5400 (Isotopx Inc.), have been able to resolve H_3 from DH, $\Delta m = 0.00155$ Da [54].

In comparing this modified Siemens Quantra FT-ICR to any one of the double-focusing magnetic sector instruments, the main disadvantage of magnetic sector instrument is its large footprint and weight, whereas the foot print of the Quantra and its manifold can be as small as 2 Ft by 5 Ft. Another advantage is that the no maintenance, internal ion pump provides the high vacuum. And over a broad mass range, a FT-ICR instrument provides the highest mass measurement accuracy (MMA) [55–57]. One disadvantage of the Siemens Quantra system is that it does not have multiple ionization methods, as only an EI ionization source is currently available [36]. A disadvantage of other FT-ICR mass spectrometers with higher resolution is that the superconducting magnets require maintenance using liquid cryogens.

4. Conclusions

Six Quantra FT-ICR mass spectrometers have been significantly upgraded to enable the high resolution, high sensitivity measurements of atomic and molecular species below 12 Da. As described within the Supporting Information, the enhancements included an external AWG and DSO, a cable panel, and an Arduino microprocessor. A LabVIEW program has been used for both instrument operation and spectrum acquisition. In addition, an all metal sample preparation system, constructed to UHV standards, has been developed that was also controlled by the LabVIEW program. The calibration curves for ^{3}He, ^{4}He, ^{20}Ne, and ^{40}Ar show excellent linearity and quantification capability down to a LLOQ of 1.5 pmole and below. The addition of a layered cryotrap greatly improves the dynamic range of the Quantra for ^{4}He determinations if sampling above aqueous solutions are involved, or if air intrusion into the sample has occurred. Future enhancements and upgrades are planned to improve the sensitivity, the resolution, and the robustness of this mass spectrometer, and to extend into quantitative measurements of tritium with sub-picomole sensitivity.

Declaration of competing interest

The authors declare that they have no known competing financial interests or personal relationships that could have appeared to influence the work reported in this paper.

Acknowledgement

The authors would like to thank the Texas Tech physics shop for their technical assistance and useful discussions. A special thanks to Dr. Steven C. Beu (S C Beu Consulting, Austin, TX) for extensive contributions as a consultant on this effort to the instrument design and in the LabView software development. We thank Chase Mulligan, Nicholas Elsaesser, Madison Atwood, Jared Rauch, and Jonathan Moore for providing assembly and mechanical design and fabrication services. This work was supported by the Texas Research Incentive Program and Texas Tech University. Identification of commercial products used in this work is for documentation purposes, and does not imply any recommendation or endorsement by Texas Tech University or our affiliates.

Appendix A. Supplementary data

Supplementary data to this article can be found online at https://doi.org/10.1016/j.ijms.2021.116574.

References

[1] E. Gluckauf, A micro-analysis of the helium and neon contents of air, Proc. Roy. Soc. Lond. Math. Phys. Sci. 185 (1000) (1946) 98–119, https://doi.org/10.1098/rspa.1946.0007.
[2] NOAA, NASA, USAF, U.S. Standard Atmosphere, U.S. Government Printing Office, Washington, DC, 1976, 1976.
[3] G. Kockarts, Helium in the terrestrial atmosphere, Space Sci. Rev. 14 (6) (1973) 723–757, https://doi.org/10.1007/BF00224775.
[4] M. Ozima, F.A. Podosek, Noble Gas Geochemistry, second ed., Cambridge University Press, Cambridge, 2001 https://doi.org/10.1017/CBO9780511545986.
[5] B.D. Shizgal, G.G. Arkos, Nonthermal escape of the atmospheres of venus, earth, and mars, Rev. Geophys. 34 (4) (1996) 483–505, https://doi.org/10.1029/96RG02213.
[6] Y. Sano, H. Wakita, Y. Makide, T. Tominaga, A ten-year decrease in the atmospheric helium isotope ratio possibly caused by human activity, Geophys. Res. Lett. 16 (12) (1989) 1371–1374, https://doi.org/10.1029/GL016i012p01371.
[7] T.A. Davidson, D.E. Emerson, Direct determination of the helium 3 content of atmospheric air by mass spectrometry, J. Geophys. Res.: Atmosphere 95 (D4) (1990) 3565–3569, https://doi.org/10.1029/JD095iD04p03565.
[8] J.H. Hoffman, A.O. Nier, Atmospheric helium isotopic ratio, Geophys. Res. Lett. (1993), https://doi.org/10.1029/93GL00112.
[9] J. Lupton, L. Evans, The atmospheric helium isotope ratio: is it changing? Geophys. Res. Lett. 31 (13) (2004) 1–4, https://doi.org/10.1029/2004GL020041.
[10] J. Lupton, L. Evans, Changes in the atmospheric helium isotope ratio over the

past 40 years, Geophys. Res. Lett. 40 (23) (2013) 6271–6275, https://doi.org/10.1002/2013GL057681.
[11] P.W. Holland, D.E. Emerson, A determination of the helium 4 content of near-surface atmospheric air within the continental United States, J. Geophys. Res.: Solid Earth 92 (B12) (1987) 12557–12566, https://doi.org/10.1029/JB092iB12p12557.
[12] P. Jean-Baptiste, E. Fourré, P. Cassette, New determination of the ^{3}He mixing ratio in the Earth's lower atmosphere from an international tritium intercomparison exercise, Appl. Geochem. 98 (July) (2018) 17–21, https://doi.org/10.1016/j.apgeochem.2018.09.003.
[13] C. Boucher, T. Lan, J. Mabry, D.V. Bekaert, P.G. Burnard, B. Marty, Spatial analysis of the atmospheric helium isotopic composition: geochemical and environmental implications, Geochem. Cosmochim. Acta 237 (2018) 120–130, https://doi.org/10.1016/j.gca.2018.06.010.
[14] C. Boucher, B. Marty, L. Zimmermann, R. Langenfelds, Atmospheric helium isotopic ratio from 1910 to 2016 recorded in stainless steel containers, Geochemical Perspectives Letters 6 (2017) 23–27, https://doi.org/10.7185/geochemlet.1804, 2017.
[15] J. Mabry, T. Lan, P. Burnard, B. Marty, High-precision helium isotope measurements in air, J. Anal. At. Spectrom. 28 (12) (2013) 1903–1910, https://doi.org/10.1039/c3ja50155h.
[16] J.C. Mabry, T. Lan, C. Boucher, P.G. Burnard, M.S. Brennwald, R. Langenfelds, B. Marty, No evidence for change of the atmospheric helium isotope composition since 1978 from re-analysis of the Cape Grim Air Archive, Earth Planet Sci. Lett. 428 (2015) 134–138, https://doi.org/10.1016/j.epsl.2015.07.035.
[17] D. Györe, A. Tait, D. Hamilton, F.M. Stuart, The formation of NeH^{+} in static vacuum mass spectrometers and re-determination of $^{21}Ne/^{20}$ of air, Geochem. Cosmochim. Acta 263 (2019) 1–12, https://doi.org/10.1016/j.gca.2019.07.059.
[18] J.M. Saxton, The $^{21}Ne/^{20}$ ratio of atmospheric neon, J. Anal. At. Spectrom. 35 (5) (2020) 943–952, https://doi.org/10.1039/d0ja00031k.
[19] D. Wielandt, M. Storey, A new high precision determination of the atmospheric ^{21}Ne abundance, J. Anal. At. Spectrom. 34 (3) (2019) 535–549, https://doi.org/10.1039/c8ja00336j.
[20] M. Honda, X. Zhang, D. Phillips, D. Hamilton, M. Deerberg, J.B. Schwieters, Redetermination of the ^{21}Ne relative abundance of the atmosphere, using a high resolution, multi-collector noble gas mass spectrometer (HELIX-MC Plus), Int. J. Mass Spectrom. 387 (2015) 1–7, https://doi.org/10.1016/j.ijms.2015.05.012.
[21] Y. Arata, Y.-C. Zhang, Observation of anomalous heat release and helium-4 production from highly deuterated palladium fine particles, Jpn. J. Appl. Phys. 38 (Part 2, No. 7A) (1999) L774–L776, https://doi.org/10.1143/jjap.38.l774.
[22] M.H. Miles, R.A. Hollins, B.F. Bush, J.J. Lagowski, R.E. Miles, Correlation of excess power and helium production during D_2O and H_2O electrolysis using palladium cathodes, J. Electroanal. Chem. 346 (1–2) (1993) 99–117, https://doi.org/10.1016/0022-0728(93)85006-3.
[23] J.R. Morrey, M.W. Caffee, H. Farrar, N.J. Hoffman, G.B. Hudson, R.H. Jones, M.D. Kurz, J. Lupton, B.M. Oliver, B.V. Ruiz, J.F. Wacker, A. van Veen, Measurements of helium in electrolyzed palladium, Fusion Technol. 18 (4) (1990) 659–668, https://doi.org/10.13182/FST90-A29260.
[24] B.F. Bush, J.J. Lagowski, M.H. Miles, G.S. Ostrom, Helium production during the electrolysis of D_2O in cold fusion experiments, J. Electroanal. Chem. 304 (1–2) (1991) 271–278, https://doi.org/10.1016/0022-0728(91)85510-V.
[25] W.B. Clarke, Search for ^{3}He and ^{4}He in arata-style palladium cathodes I: a negative result, Fusion Sci. Technol. 40 (2) (2001) 147–151, https://doi.org/10.13182/FST01-A189.
[26] W.B. Clarke, B.M. Oliver, M.C.H. McKubre, F.L. Tanzella, P. Tripodi, Search for ^{3}He and ^{4}He in arata-style palladium cathodes II: evidence for tritium production, Fusion Sci. Technol. 40 (2) (2001) 152–167, https://doi.org/10.13182/FST01-A190.
[27] R. Nachtrieb, B. LaBombard, E. Thomas, Omegatron ion mass spectrometer for the Alcator C-mod tokamak, Rev. Sci. Instrum. 71 (11) (2000) 4107–4118, https://doi.org/10.1063/1.1311942.
[28] D. Brunner, B. LaBombard, R. Ochoukov, D. Whyte, Scanning retarding field analyzer for plasma profile measurements in the boundary of the Alcator C-Mod tokamak, Rev. Sci. Instrum. 84 (3) (2013), https://doi.org/10.1063/1.4793785.
[29] C.C. Klepper, T.M. Biewer, U. Kruezi, S. Vartanian, D. Douai, D.L. Hillis, C. Marcus, Extending helium partial pressure measurement technology to JET DTE2 and ITER, Rev. Sci. Instrum. 87 (11) (2016), https://doi.org/10.1063/1.4963713.
[30] S. Davies, J.A. Rees, D.L. Seymour, Threshold ionisation mass spectrometry (TIMS); A complementary quantitative technique to conventional mass resolved mass spectrometry, Vacuum 101 (2014) 416–422, https://doi.org/10.1016/j.vacuum.2013.06.004.
[31] D. Alegre, T.J. Finlay, J.W. Davis, A.A. Haasz, F.L. Tabarés, Oxidative removal of tokamak codeposits using NO_2 and O_2, J. Nucl. Mater. 438 (SUPPL) (2013) S1104–S1108, https://doi.org/10.1016/j.jnucmat.2013.01.243.
[32] Y. Yu, J. Hu, Z. Wan, J. Wu, H. Wang, B. Cao, Mass separation of deuterium and helium with conventional quadrupole mass spectrometer by using varied ionization energy, Rev. Sci. Instrum. 87 (3) (2016) 1–5, https://doi.org/10.1063/1.4944560.
[33] W.A. Spencer, L.L. Tovo, Siemens Advanced Quantra Fticr Mass Spectrometer for Ultra High Resolution at Low Mass, Tech. Rep. WSRC-STI-2008-00161, Analytical Development Section, Savannah River National Laboratory, 2008, https://doi.org/10.2172/935437.
[34] W.A. Brand, T.B. Coplen, An interlaboratory study to test instrument performance of hydrogen dual-inlet isotope-ratio mass spectrometers, Fresenius' J. Anal. Chem. 370 (4) (2001) 358–362, https://doi.org/10.1007/s002160100814.
[35] W.B. Chastagner, P. Daves, H.L. Hess, Advanced mass spectrometers for hydrogen isotope analyses, Int. J. Mass Spectrom. Ion Phys. 48 (1983) 353–356, https://doi.org/10.1016/0020-7381(83)87100-9.
[36] W. Davis, D.V. Kania, A. Rimkus, Fourier transform mass spectrometers - new developments in process analysis, Atp-Edition: automatisierungstechnische Praxis 44 (5) (2002) 53–57.
[37] M. Heninger, H. Mestdagh, E. Louarn, G. Mauclaire, P. Boissel, J. Leprovost, E. Bauchard, S. Thomas, J. Lemaire, Gas analysis by electron ionization combined with chemical ionization in a compact FTICR mass spectrometer, Anal. Chem. 90 (12) (2018) 7517–7525, https://doi.org/10.1021/acs.analchem.8b01107.
[38] S. Thomas, N. Blin-Simiand, M. Héninger, P. Jeanney, J. Lemaire, L. Magne, H. Mestdagh, S. Pasquiers, E. Louarn, Direct and real-time analysis in a plasma reactor using a compact FT-ICR MS: degradation of acetone in nitrogen and byproduct formation, J. Am. Soc. Mass Spectrom. 31 (7) (2020) 1579–1586, https://doi.org/10.1021/jasms.0c00141.
[39] G. Mauclaire, J. Lemaire, P. Boissel, G. Bellec, M. Heninger, MICRA: a compact permanent magnet Fourier transform ion cyclotron resonance mass spectrometer, Eur. J. Mass Spectrom. 10 (2 SPEC. ISS.) (2004) 155–162, https://doi.org/10.1255/ejms.620.
[40] P.J. Linstrom, W.G. Mallard, NIST Chemistry webBook, NIST Standard Reference Database Number 69, National Institute of Standards and Technology, 2014, https://doi.org/10.18434/T4D303.
[41] C. Boffito, B. Ferrario, P. della Porta, L. Rosai, Nonevaporable low temperature activatable getter material, J. Vac. Sci. Technol. 18 (3) (1980) 1117–1120, https://doi.org/10.1116/1.570852.
[42] J.H. Reynolds, P.M. Jeffery, G.A. McCrory, P.M. Varga, Improved charcoal trap for rare gas mass spectrometry, Rev. Sci. Instrum. 49 (4) (1978) 547–548, https://doi.org/10.1063/1.1135429.
[43] P.J. Hooker, R. Bertrami, S. Lombardi, R.K. O'Nions, E.R. Oxburgh, Helium-3 anomalies and crust-mantle interaction in Italy, Geochem. Cosmochim. Acta 49 (12) (1985) 2505–2513, https://doi.org/10.1016/0016-7037(85)90118-8.
[44] P.C. Meier, R.E. Zünd, Statistical Methods in Analytical Chemistry, Wiley Blackwell, 2005, https://doi.org/10.1002/0471728411.
[45] P. Burnard, L. Zimmermann, Y. Sano, The noble gases as geochemical tracers: history and background, in: P. Burnard (Ed.), Advances in Isotope Geochemistry, first ed., Springer-Verlag, Berlin Heidelberg, 2013, pp. 1–15, https://doi.org/10.1007/978-3-642-28836-4. Ch. 1.
[46] T. Porcelli, F. Siviero, G.A. Bongiorno, P. Michelato, C. Pagani, Influence of the cathode materials on the sorption of noble gases by sputter-ion pumps, Vacuum 122 (2015) 218–221, https://doi.org/10.1016/j.vacuum.2015.10.003.
[47] J. Mabry, P. Burnard, P.H. Blard, L. Zimmermann, Mapping changes in helium sensitivity and peak shape for varying parameters of a Nier-type noble gas ion source, J. Anal. At. Spectrom. 27 (6) (2012) 1012–1017, https://doi.org/10.1039/c2ja10339g.
[48] L. Junjie, L. Hanbin, Z. Jia, Ne and Ar isotope analysis of samples with high abundance ratios of Ar/Ne and low abundance of Ne by MMS and QMS, J. Anal. At. Spectrom. 34 (6) (2019) 1205–1215, https://doi.org/10.1039/c8ja00454d.
[49] D.E. Lott, W.J. Jenkins, An automated cryogenic charcoal trap system for helium isotope mass spectrometry, Rev. Sci. Instrum. 55 (12) (1984) 1982–1988, https://doi.org/10.1063/1.1137692.
[50] T. Torgersen, Terrestrial helium degassing fluxes and the atmospheric helium budget: implications with respect to the degassing processes of continental crust, Chem. Geol.: Isotope Geoscience Section (1989), https://doi.org/10.1016/0168-9622(89)90002-X.
[51] P.P. Tans, T.J. Conway, T. Nakazawa, Latitudinal distribution of the sources and sinks of atmospheric carbon dioxide derived from surface observations and an atmospheric transport model, J. Geophys. Res.: Atmosphere 94 (D4) (1989) 5151–5172, https://doi.org/10.1029/JD094iD04p05151.
[52] J. Lupton, D. Graham, Comment on "a ten-year decrease in the atmospheric helium isotope ratio possibly caused by human activity", in: y. sano, et al. (Eds.), Geophys. Res. Lett. 18 (3) (1991) 482–485, https://doi.org/10.1029/91GL00493.
[53] J.H. Reynolds, High sensitivity mass spectrometer for noble gas analysis, Rev. Sci. Instrum. 27 (11) (1956) 928–934, https://doi.org/10.1063/1.1715415.
[54] A. Ludin, R. Weppernig, G. Bonisch, P. Schlosser, Mass Spectrometric Measurement of Helium Isotopes and Tritium in Water Samples, Lamont-Doherty Earth Observatory of Columbia University, Palisades, NY, 1997.
[55] C. Masselon, A.V. Tolmachev, G.A. Anderson, R. Harkewicz, R.D. Smith, Mass measurement errors caused by 'local' frequency perturbations in FTICR mass spectrometry, J. Am. Soc. Mass Spectrom. 13 (1) (2002) 99–106, https://doi.org/10.1016/S1044-0305(01)00333-6.
[56] M.V. Gorshkov, S. Guan, A.G. Marshall, Masses of stable neon isotopes determined at parts per billion precision by Fourier transform ion cyclotron resonance mass spectrometry, Int. J. Mass Spectrom. Ion Process. 128 (1–2) (1993) 47–60, https://doi.org/10.1016/0168-1176(93)87015-K.
[57] M.L. Easterling, T.H. Mize, I.J. Amster, Routine part-per-million mass accuracy for high-mass ions: space-charge effects in MALDI FT-ICR, Anal. Chem. 71 (3) (1999) 624–632, https://doi.org/10.1021/ac980690d.